Preclinical Development

Molecular Cancer Therapeutics

Sorafenib Inhibits the Hepatocyte Growth Factor–Mediated Epithelial Mesenchymal Transition in Hepatocellular Carcinoma

Tomoyuki Nagai[1,2], Tokuzo Arao[1], Kazuyuki Furuta[1], Kazuko Sakai[1], Kanae Kudo[1,2], Hiroyasu Kaneda[1], Daisuke Tamura[1], Keiichi Aomatsu[1], Hideharu Kimura[1], Yoshihiko Fujita[1], Kazuko Matsumoto[1], Nagahiro Saijo[3], Masatoshi Kudo[2], and Kazuto Nishio[1]

Abstract

The epithelial mesenchymal transition (EMT) has emerged as a pivotal event in the development of the invasive and metastatic potentials of cancer progression. Sorafenib, a VEGFR inhibitor with activity against RAF kinase, is active against hepatocellular carcinoma (HCC); however, the possible involvement of sorafenib in the EMT remains unclear. Here, we examined the effect of sorafenib on the EMT. Hepatocyte growth factor (HGF) induced EMT-like morphologic changes and the upregulation of SNAI1 and N-cadherin expression. The downregulation of E-cadherin expression in HepG2 and Huh7 HCC cell lines shows that HGF mediates the EMT in HCC. The knockdown of SNAI1 using siRNA canceled the HGF-mediated morphologic changes and cadherin switching, indicating that SNAI1 is required for the HGF-mediated EMT in HCC. Interestingly, sorafenib and the MEK inhibitor U0126 markedly inhibited the HGF-induced morphologic changes, SNAI1 upregulation, and cadherin switching, whereas the PI3 kinase inhibitor wortmannin did not. Collectively, these findings indicate that sorafenib downregulates SNAI1 expression by inhibiting mitogen-activated protein kinase (MAPK) signaling, thereby inhibiting the EMT in HCC cells. In fact, a wound healing and migration assay revealed that sorafenib completely canceled the HGF-mediated cellular migration in HCC cells. In conclusion, we found that sorafenib exerts a potent inhibitory activity against the EMT by inhibiting MAPK signaling and SNAI1 expression in HCC. Our findings may provide a novel insight into the anti-EMT effect of tyrosine kinase inhibitors in cancer cells. *Mol Cancer Ther; 10(1); 169–77. ©2011 AACR.*

Introduction

Hepatocellular carcinoma (HCC) is the fifth most common cancer and the third largest cause of cancer-related death in the world annually (1). Recurrence, metastasis, and the development of new primary tumors are the most common causes of mortality among patients with HCC (2). Sorafenib (Nexavar; Bayer HealthCare Pharmaceuticals Inc.) is a small molecule that inhibits the kinase activities of Raf-1 and B-Raf in addition to VEGFRs, PDGFR-β (platelet-derived growth factor receptor β), Flt-3, and c-KIT (3). Two recent randomized controlled trials reported a clinical benefit of single-agent sorafenib in extending overall survival in both Western and Asian patients with advanced unresectable HCC (4, 5). The potential action mechanisms that lead to these clinical benefits are thought to include antiangiogenic effects and sorafenib's characteristic inhibitory effect on Raf-1 and B-Raf signaling.

Meanwhile, growing evidence indicates that the epithelial mesenchymal transition (EMT), a developmental process by which epithelial cells reduce intercellular adhesions and acquire fibroblastoid properties, has important roles in the development of the invasive and metastatic potentials of cancer progression (6–8). To date, numerous clinicopathologic studies have shown positive correlations between the expressions of the transcription factors SNAI1 (snail homologue 1/SNAIL) and SNAI2 (snail homologue 2/Slug), which are key inducible factors of the EMT, and poor clinical outcomes in breast, ovary, colorectal, and lung cancer; squamous cell carcinoma; melanoma, and HCC (reviewed in ref. 6).

Generally, the activation of a wide variety of ligands including FGF (fibroblast growth factor), TGF-β–BMPs (bone morphogenetic protein), Wnt, EGF (epidermal growth factor), VEGF, and HGF (hepatocyte growth factor) and its receptor can upregulate the expression of EMT-regulating transcription factors, including SNAI1, SNAI2, ZEB1, ZEB2, and TWIST (6). Among them, HGF (also known as scattering factor) activates

Authors' Affiliations: Departments of [1]Genome Biology, [2]Gastroenterology and [3]Medical Oncology, Kinki University School of Medicine, Japan

Note: Supplementary material for this article is available at Molecular Cancer Therapeutics Online (http://mct.aacrjournals.org/).

Corresponding Author: Kazuto Nishio, Department of Genome Biology, Kinki University School of Medicine, 377-2 Ohno-higashi, Osaka-Sayama, Osaka 589-8511, Japan. Phone: 81-72-366-0221 (ext 3150); Fax: 81-72-367-6369; E-mail: knishio@med.kindai.ac.jp

doi: 10.1158/1535-7163.MCT-10-0544

the Met signaling pathway, thereby increasing the invasive and metastatic potentials of the cells and allowing the survival of cancer cells in the bloodstream in the absence of anchorage (9). In addition, HGF is well known as a potent angiogenic cytokine, and Met signal activation can modify the microenvironment to facilitate cancer progression (9). Therefore, the HGF-Met signaling pathway is regarded as a promising therapeutic target, and many molecular targeted drugs are under clinical development (10). In HCC, the mRNA levels of HGF and Met receptor are markedly increased compared with those in normal liver (11). A high serum HGF concentration is associated with a poor prognosis for overall survival after hepatic resection, and the serum level of HGF represents the degree of the carcinogenic state in the livers of patients with C-viral chronic hepatitis and cirrhosis (12–14). Thus, we examined the effect of sorafenib on the HGF-Met–mediated EMT in HCC.

Materials and Methods

Reagents

Sorafenib was provided by Bayer HealthCare Pharmaceuticals Inc. U0126, wortmannin (Cell Signaling Technology), and human HGF (R&D Systems) were purchased from the indicated companies. The structures of compounds are shown in Supplementary Figure 1.

Cell culture

The human HCC cell lines HepG2 and Huh7 were maintained in Dulbecco's modified Eagle's (DMEM) medium (Sigma) supplemented with 10% FBS, penicillin, and streptomycin (Sigma) in a humidified atmosphere of 5% CO_2 at 37°C. The cell lines were obtained from the Japanese Collection of Research Bioresources and were grown in culture for less than 6 months.

Scratch assay

The method used for the scratches assay has been previously described (15). Briefly, the cells were plated onto 24-well plates and incubated in DMEM containing 10% FBS until they reached subconfluence. Scratches were introduced to the subconfluent cell monolayer, using a plastic pipette tip. The cells were then cultured with DMEM containing 10% FBS at 37°C. After 24 hours, the scratch area was photographed using a light microscope (IX71; Olympus). The wound distance between edge to edge were measured and averaged from 5 points per 1 wound area, using DP manager software (Olympus). The 2 wound areas were evaluated in an experiment and the experiment was done in triplicate.

Migration assay

The migration assays were done using the Boyden chamber methods and polycarbonate membranes with an 8-μm pore size (Chemotaxicell), as previously described (15). The membranes were coated with fibronectin on the outer side and dried for 2 hours at room temperature. The cells to be analyzed (2×10^4 cells/well) were then seeded onto the upper chambers with 200 μL of migrating medium (DMEM containing 0.5% FBS), and the upper chambers were placed into the lower chambers of 24-well culture dishes containing 600 μL of DMEM containing 10% FBS or with 10 ng/mL of HGF or with HGF and 10 μmol/L of sorafenib. After incubation for 36 hours (HepG2) and 24 hours (Huh7), the media in the upper chambers were aspirated and the nonmigrated cells on the inner sides of the membranes were removed using a cotton swab. The cells that had migrated to the outer side of the membranes were fixed with 4% paraformaldehyde for 10 minutes, stained with 0.1% Giemsa stain solution for 15 minutes, and then counted using a light microscope. Migrated cells were averaged from 5 fields per 1 chamber and 3 chambers were used on 1 experiment. The experiment was done in triplicate.

Morphologic analysis

HepG2 and Huh7 cells (2×10^4 and 1×10^4 cells/well, respectively) were seeded in 6-well tissue culture dishes. After 24 hours of incubation, the cells were stimulated with 10 ng/mL of HGF or control PBS. When the inhibitors were used, the cells were exposed to each inhibitor for 3 hours before the addition of HGF. After 48 hours, the cells were analyzed using a light microscope. The experiment was done in triplicate.

Western blot analysis

The following antibodies were used in this study: phospho-Met (Y1349), Met, phospho-AKT (S473), AKT, phospho-p44/42 mitogen-activated protein kinase (MAPK), SNAI1/Snail, E-cadherin, N-cadherin, vimentin, β-actin antibody horseradish peroxidase–conjugated secondary antibody (Cell Signaling Technology), and fibronectin (Santa Cruz Biotechnology). All the experiments were done at least in duplicate. The Western blot analysis was done as described previously (16). The data were quantified by automated densitometry using Multigauge Ver. 3.0 (Fujifilm). Densitometric data were normalized by β-actin in triplicate and the average was shown above the Western blot as a ratio of control sample.

Real-time reverse transcription PCR

The real-time reverse transcription PCR (RT-PCR) method has been previously described (17). Briefly, 1 μg of total RNA from the cultured cells was converted to cDNA using a GeneAmp RNA-PCR kit (Applied Biosystems). Real-time RT-PCR amplification was done using a Thermal Cycler Dice (Takara) in accordance with the manufacturer's instructions under the following conditions: 95°C for 6 minutes, 40 cycles of 95°C for 15 seconds, and 60°C for 1 minute. Glyceraldehyde 3-phosphate dehydrogenase (GAPD) was used to normalize the expression levels in the subsequent quantitative analyses. To amplify the target genes, the following primers were purchased from TaKaRa: *CDH1*, forward 5′-TTA AAC

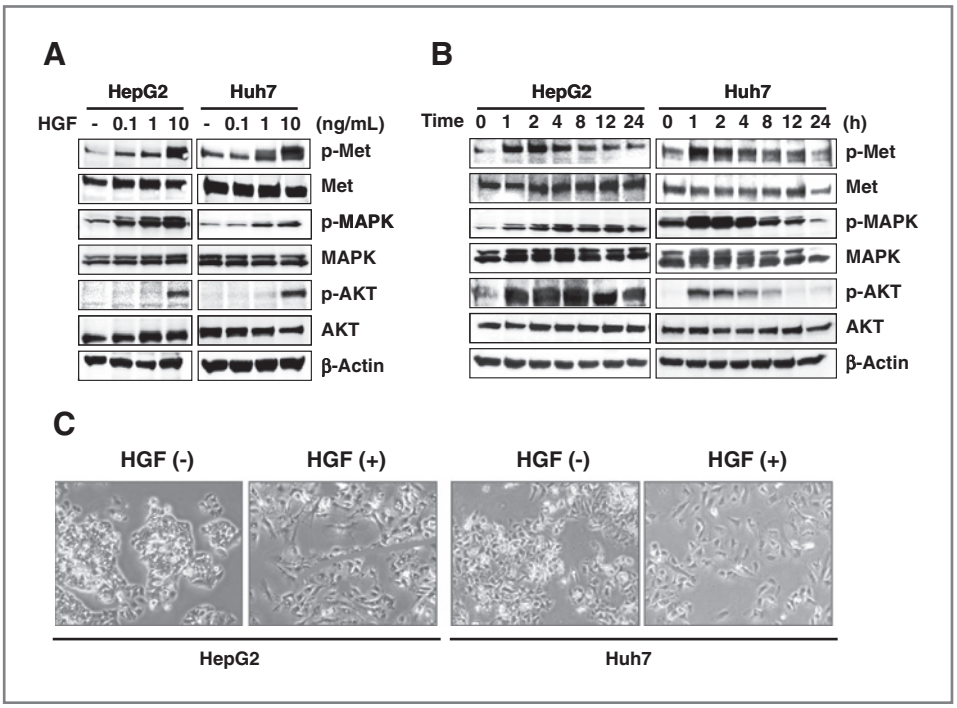

Figure 1. HGF stimulates the Met signaling pathway and induces morphologic changes in HCC. A, HGF stimulation (0, 0.1, 1, and 10 ng/mL) dose-dependently increased the phosphorylation of Met, MAPK, and AKT in the HCC cell lines HepG2 and Huh7. The results of a Western blot analysis are shown. β-Actin was used as a loading control. The serum-starved cells were stimulated with HGF for 60 minutes and then collected for analysis. B, time-course analysis of HGF stimulation. The HCC cells were stimulated with 10 ng/mL of HGF for 0, 1, 2, 4, 8, 12, and 24 hours. The results of a Western blot analysis are shown. C, HGF-mediated morphologic changes included cell scattering and the elongation of the cell shape that are characteristic of the EMT. The HepG2 and Huh7 cells were stimulated with or without 10 ng/mL of HGF for 48 hours and then photographed (magnification × 200).

TCC TGG CCT CAA GCA ATC-3′ and reverse 5′-TCC TAT CTT GGG CAA AGC AAC TG-3′; *CDH2*, forward 5′-CGA ATG GAT GAA AGA CCC ATC C-3′ and reverse 5′-GGA GCC ACT GCC TTC ATA GTC AA-3'; *SNAI1*, forward 5′-TCT AGG CCC TGG CTG CTA CAA-3′ and reverse 5′-ACA TCT GAG TGG GTC TGG AGG TG-3′; *SNAI2*, forward 5′-ATG CAT ATT CGG ACC CAC ACA TTA C-3′ and reverse 5′-AGA TTT GAC CTG TCT GCA AAT GCT C-3′; *VIM*, forward 5′-TGA GTA CCG GAG ACA GGT GCA G-3′ and reverse 5′-TAG CAG CTT CAA CGG CAA AGT TC-3′; *FN1*, forward 5′-GGA GCA AAT GGC ACC GAG ATA-3′ and reverse 5′-GAG CTG CAC ATG TCT TGG GAA C-3′; and *GAPD*, forward 5′-GCA CCG TCA AGG CTG AGA AC-3′ and reverse 5′-ATG GTG GTG AAG ACG CCA GT-3′.

Small interfering RNA transfection

Three different sequences of small interfering RNA (siRNA) targeting human SNAI1 (Hs_SNAI1_9785, 9786, and 9787) and those of 2 scramble control siRNAs were purchased from Sigma Aldrich Japan. The transfection methods have been previously described (17).

Statistical analysis

The statistical analyses were done using Microsoft Excel (Microsoft) both to calculate the SD and to test for statistically significant differences between the samples using a Student t test. A value $P < 0.05$ was considered statistically significant.

Results

To examine the activity of HGF-Met signaling in HCC cells, we examined the expressions of phospho-Met, Met, phospho-AKT, AKT, phospho-MAPK, and MAPK in the HepG2 and Huh7 cell lines, using Western blotting. The phosphorylation levels of Met, AKT, and MAPK were dose-dependently increased by HGF stimulation (Fig. 1A). A time-course analysis showed that the phosphorylation levels of Met, AKT, and MAPK peaked at 1 to 2 hours after HGF stimulation and gradually recovered to the baseline values at 4 hours later (Fig. 1B). These results indicated that Met signaling is actually capable of being activated in response to HGF in HCC cells.

From a morphologic aspect, the EMT is characterized by an increase in cell scattering and an elongation of the cell shape (18). To evaluate whether HGF mediates the morphologic change that is characteristic of the EMT in HCC cells, cellular morphology was examined after HGF stimulation. HGF clearly mediated both cell scattering and the elongation of the cell shape in HepG2 and Huh7 cell lines (Fig. 1C). These data indicate that HGF mediates

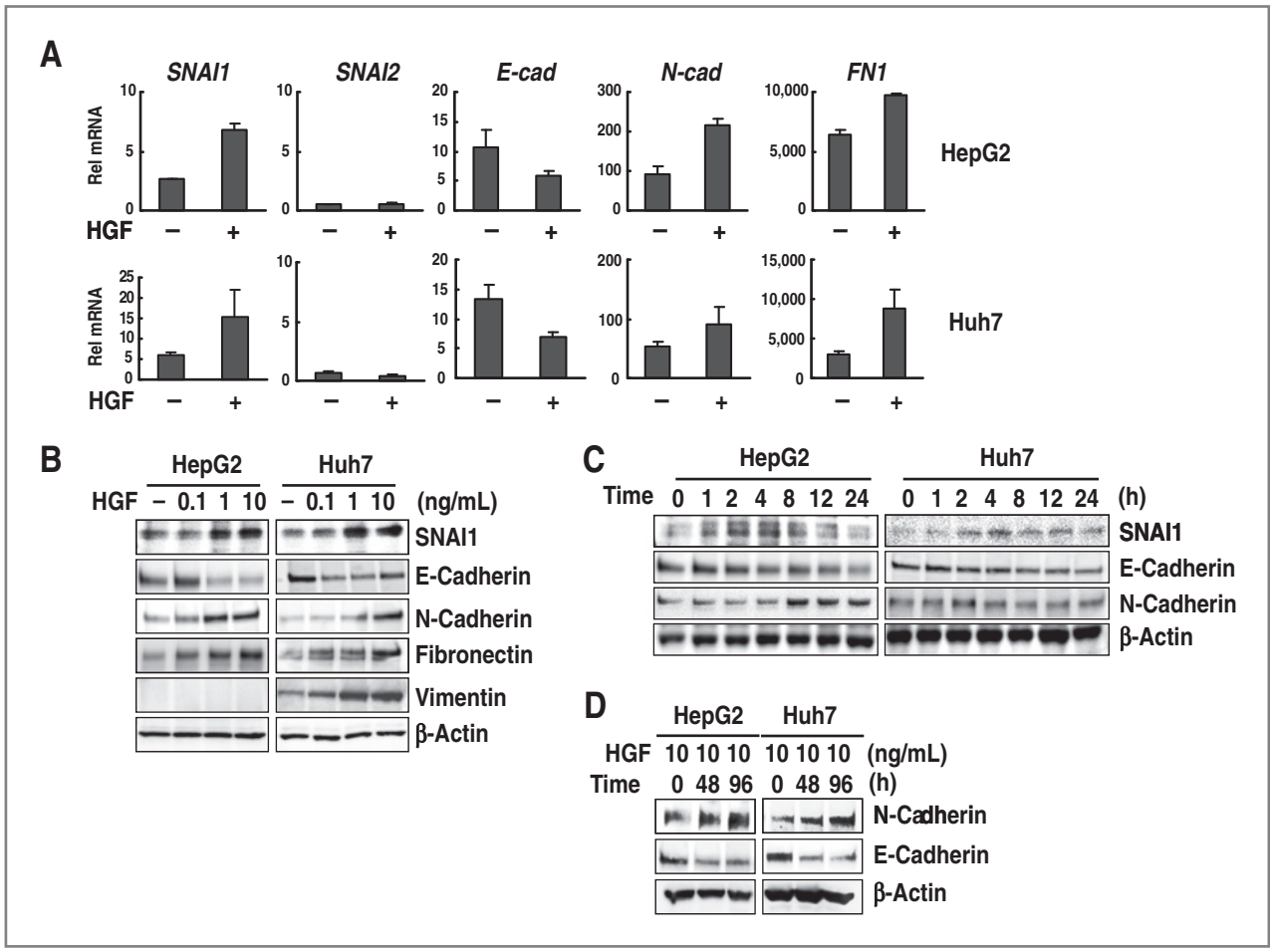

Figure 2. HGF upregulates SNAI1 expression and induces cadherin switching in HCC. A, changes in the mRNA expressions of the EMT-related genes *SNAI1/Snail*, *SNAI2/Slug*, *E-cadherin/CDH1*, *N-cadherin/CDH2*, and *fibronectin/FN1* were determined using real-time RT-PCR. The HepG2 and Huh7 cells were stimulated with or without 10 ng/mL of HGF for 2 hours (SNAI1 and SNAI2) or 48 hours (*E-cad*, *N-cad*, and *FN1*). Rel mRNA, normalized mRNA expression levels (target genes/GAPD $\times$ 10^4); E-cad, E-cadherin; N-cad, N-cadherin. B, the HGF-mediated protein expression changes in SNAI1, E-cadherin, N-cadherin, fibronectin, and vimentin were determined using a Western blot analysis. The HepG2 and Huh7 cells were stimulated with HGF at the indicated dose (0, 0.1, 1, or 10 ng/mL) and collected for analysis after 4-hour stimulation for SNAI1 and 72 hours for the others. C, the cells were stimulated with 10 ng/mL of HGF for the indicated time course (0, 1, 2, 4, 8, 12, or 24 hours) and used for analysis. β-Actin was used as a loading control. D, Western blot analysis of E-cadherin and N-cadherin. The cells were stimulated with 10 ng/mL of HGF for 0, 48, and 96 hours and then analyzed.

the morphologic changes that are compatible with the induction of the EMT in HCC cell lines.

Because SNAI1 and SNAI2 are considered to be master regulators of the EMT, changes in the mRNA expression levels of EMT-related genes in response to HGF stimulation were evaluated using real-time RT-PCR (Fig. 2A). HGF stimulation upregulated SNAI1 mRNA expression by more than 2-fold, whereas the baseline expression of SNAI2 was very low compared with that of SNAI1 and did not respond to HGF in either of the HCC cell lines that were examined. Cadherin switching, which is characterized by the downregulation of E-cadherin and the upregulation of N-cadherin, is known as one of the most pivotal cellular events in the EMT (19). Cadherin switching was clearly observed on the basis of mRNA levels after HGF stimulation. The mesenchymal marker fibronectin was also upregulated (Fig. 2A).

Consistent with the mRNA changes, HGF stimulation dose-dependently upregulated the protein expression of SNAI1, N-cadherin, fibronectin, and vimentin and downregulated the expression of E-cadherin in both cell lines (Fig. 2B). Vimentin expression of HepG2 was not detected (baseline vimentin mRNA was also extremely low; data not shown). A time-course analysis showed that HGF upregulated the SNAI1 expression at 2 hours after stimulation and that the expression level recovered to the baseline value at 24 hours thereafter (Fig. 2C). Cadherin switching after HGF stimulation was observed at 8 hours later in HepG2 cells and 48 hours later in Huh7 cells (Fig. 2C and D). Generally, upregulation of SNAI1 is

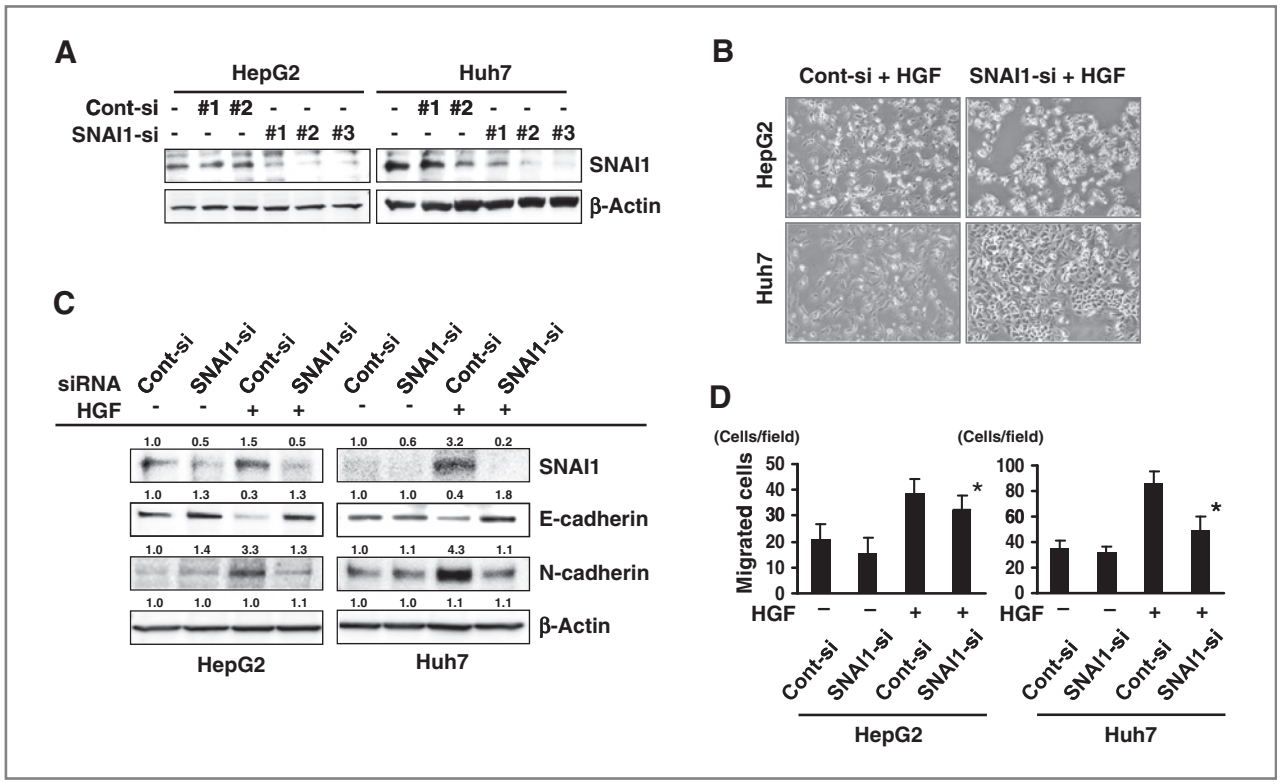

Figure 3. SNAI1 is required to induce the HGF-mediated EMT in HCC cells. A, knockdown of HGF-mediated SNAI1 expression using siRNA. Three sequences of SNAI1-siRNA (1, 2, and 3) were used. The HepG2 and Huh7 cells were treated with or without 50 nmol/L of each siRNA for 48 hours and then were stimulated with 10 ng/mL of HGF. SNAI1-siRNA #2 was effective and was used in subsequent experiments. B, SNAI1 knockdown canceled the HGF-mediated morphologic changes. The HepG2 and Huh7 cells were treated with 50 nmol/L of siRNA for 48 hours and were then stimulated with 10 ng/mL of HGF in all 4 panels. C, SNAI1 suppression by siRNA strongly canceled the HGF-mediated downregulation of E-cadherin and the upregulation of N-cadherin in both HepG2 and Huh7 cells. The cells were treated with 50 nmol/L of siRNA for 48 hours and were analyzed using a Western blot analysis. Densitometric data are shown above the Western blot. D, the siRNA knockdown of SNAI1 inhibited the HGF-mediated cellular migration. The siRNA-transfected HepG2 and Huh7 cells were evaluated using migration assay. The migration assays were conducted using the Boyden chamber methods as described in Materials and Methods. *, $P < 0.05$ (Cont-si vs. SNAI1-si with HGF); Cont-si, control-siRNA; SNAI1-si, SNAI1-targeting siRNA.

observed within few hours, but cadherin switching occurs around 24 hours later after stimulation (20, 21), consistent with our result. These results indicate that HGF meditates the induction of SNAI1, cadherin switching, and the EMT in HCC cells.

Besides SNAI1 and SNAI2, other transcription factors of several genes also have the potential to repress E-cadherin and to induce the EMT; these factors include ZEB1/TCF8, ZEB2/SMAD interacting protein 1, TWIST, E47/TCF3, and TCF4/E2-2 (6). Therefore, we examined whether SNAI1, among several EMT-inducible genes, has a central role in the HGF-mediated EMT in HCC cells. Three sequences of SNAI1-siRNA (1, 2, and 3) were used. A Western blot showed that both sequences 2 and 3 of SNAI1-siRNA completely suppressed the HGF-mediated upregulation of SNAI1 in the HepG2 and Huh7 cells (Fig. 3A); thus, the #2 SNAI1-siRNA was used in the following experiments: The siRNA knockdown of SNAI1 canceled the morphologic changes observed in HepG2 cells undergoing HGF-mediated EMT, whereas the control-siRNA did not (Fig. 3B). Similar results were obtained in Huh7 cells, indicating that SNAI1 is required for the morphologic changes observed in HGF-mediated EMT. Similarly, the siRNA knockdown of SNAI1 strongly canceled the HGF-mediated downregulation of E-cadherin and the upregulation of N-cadherin in both HepG2 and Huh7 cells (Fig. 3C). Those of mRNA expression changes were relatively correlated with the results of Western blot, except for N-cadherin in Huh7 cells (Supplementary Fig. 2A). Regarding the cellular migration, the siRNA knockdown of SNAI1 inhibited the HGF-mediated cellular migration (Fig. 3D). Collectively, these results indicate that SNAI1 is required to induce the HGF-mediated EMT in HCC cells.

In general, SNAI1 expression is regulated by ligand-receptor signal transduction through a downstream signal pathway that includes the Smad, MAPK, AKT, and GSK3 pathways (6, 22, 23). Sorafenib has been shown to inhibit RAF-MAPK signaling in HCC cells (24). Accordingly, we hypothesized that sorafenib might downregulate SNAI1 expression by inhibiting RAF-MAPK signaling, which is a unique activity of sorafenib. As

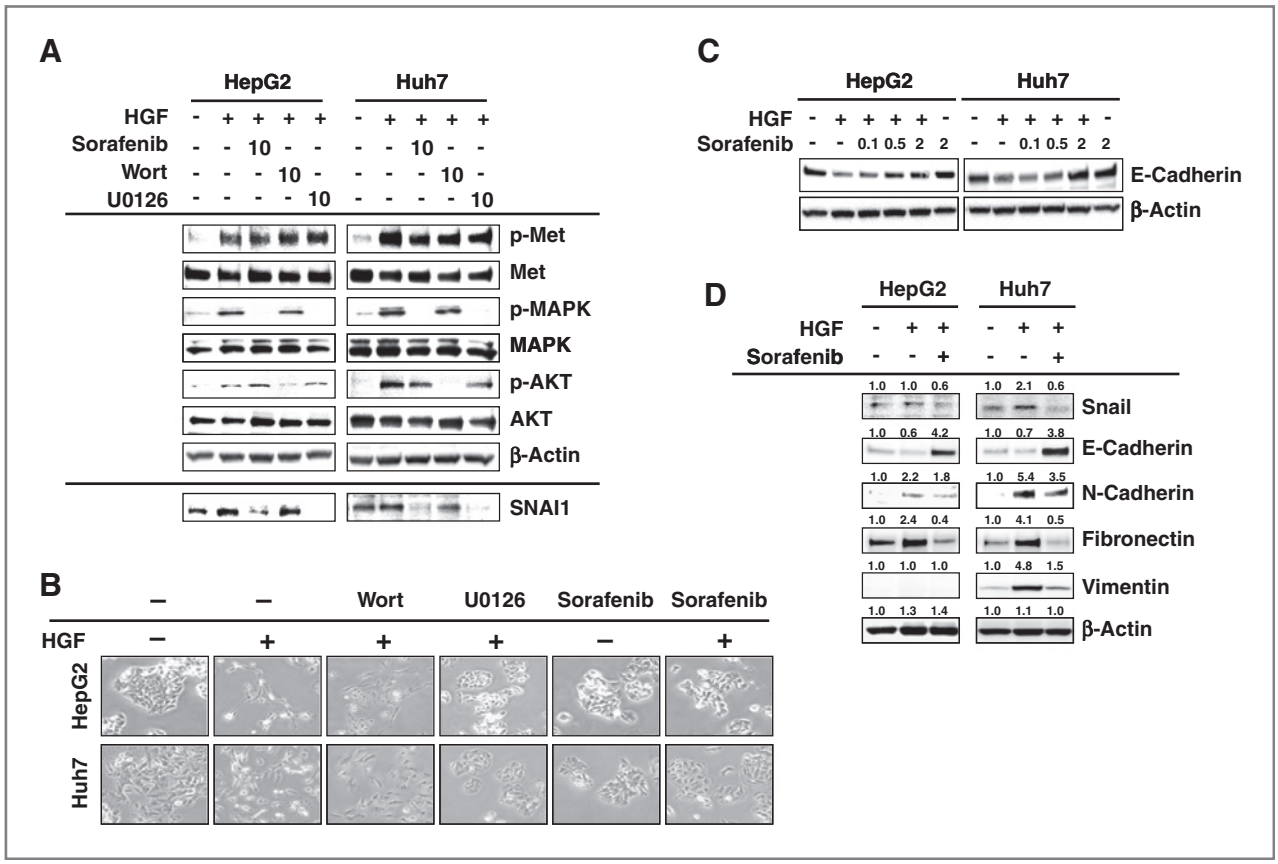

Figure 4. Sorafenib downregulates SNAI1 expression in HCC. A, as expected, sorafenib and the MEK inhibitor U0126 inhibited the HGF-mediated phosphorylation of MAPK, but the PI3K inhibitor wortmannin did not. Of note, SNAI1 expression was markedly downregulated by sorafenib and U0126. The HepG2 and Huh7 cells were exposed to 10 μmol/L of sorafenib or wortmannin or U0126 for 3 hours and were then stimulated with 10 ng/mL of HGF for 60 minutes. Wort, wortmannin. B, the HGF-mediated morphologic changes were canceled by sorafenib and U0126 but not by wortmannin in the HCC cells. The cells were exposed to sorafenib or wortmannin or U0126 for 48 hours with or without HGF (10 ng/mL) and then photographed. C, HGF-mediated downregulation of E-cadherin was canceled by sorafenib. The cells were stimulated with HGF (10 ng/mL) and treated with sorafenib at indicated concentration for 48 hours. D, HGF-mediated cadherin switching and upregulation of fibronectin and vimentin were canceled by sorafenib in the HCC cell lines. The cells were cultured with or without 2 μmol/L of sorafenib for 72 hours, with or without HGF (10 ng/mL), and then were analyzed using Western blot analysis. Densitometric data are shown above the Western blot.

expected, sorafenib and the MEK inhibitor U0126 (10 μmol/L) markedly inhibited the HGF-induced phosphorylation of MAPK, but the PI3K inhibitor wortmannin (10 μmol/L) did not. In contrast, only wortmannin inhibited the phosphorylation of AKT (Fig. 4A). Notably, SNAI1 expression was strongly downregulated by sorafenib and U0126 but not by wortmannin (Fig. 4A). These results showed that sorafenib downregulated SNAI1 expression via MAPK signaling. Meanwhile, we examined the HGF- and sorafenib-mediated expression changes of *SNAI2*, *ZEB1*, *ZEB2*, and *TWIST* using real-time RT-PCR and Western blot (Supplementary Fig. 3). Baseline and expression changes of SNAI2 and TWIST were very low compared with SNAI1, and the expression changes of ZEB1 and ZEB2 seemed not to be significant. Collectively, we considered that SNAI2, TWIST, ZEB1, and ZEB2 are not likely to be involved in the effect of HGF and sorafenib on EMT in this cell lines. Then, we examined the activity of sorafenib on HGF-mediated morphologic changes in HCC cells. HGF stimulation mediated the cell scattering and spindle-shaped changes, and these effects were clearly canceled by sorafenib and U0126, but not by wortmannin, in both HepG2 and Huh7 cells (Fig. 4B). These results were consistent with the results of Western blotting. To show whether sorafenib cancels the effect of HGF-mediated downregulation of E-cadherin, we examined the Western blot in dose–response analysis. Downregulation of E-cadherin was clearly canceled by sorafenib in a dose-dependent manner (Fig. 4C). Time-course analysis showed that HGF-mediated downregulation of E-cadherin was also canceled by sorafenib (Supplementary Fig. 4). HGF stimulation downregulated E-cadherin expression and upregulated N-cadherin, vimentin, and fibronectin in HCC cells; however, these effects were canceled by sorafenib in both HCC cell lines (Fig. 4D and Supplementary Fig. 2B). The mRNA data of N-cadherin in Huh7 cells were not correlated with protein level. These results show that sorafenib inhibits the

RAF-MAPK pathway, thereby downregulating SNAI1 and inhibiting the EMT in HCC.

Because sorafenib inhibits the HGF-mediated EMT in HCC cells, we next examined whether the inhibitory effect of sorafenib on the EMT leads to an inhibition of cellular migration in HCC cells. A scratch assay revealed that HGF stimulation increased cellular migration by about 2- fold in both HCC cell lines; however, sorafenib significantly inhibited this effect to the baseline levels (Fig. 5A). Similarly, a migration assay using the Boyden chamber method revealed that sorafenib canceled HGF-mediated cellular migration in both cell lines (Fig. 5B). These results suggest that sorafenib actually inhibits the cellular migrating phenotype of the EMT in HCC cells. The combination of migration data with siRNA and sorafenib (Fig. 3D and Fig. 5B) suggests that inhibitory effects of sorafenib on migration may be mediated by Snail downregulation in some tumors (e.g., Huh7) but not in others (e.g., HepG2). It is assumed that the inhibitory activity of sorafenib on the cellular migrating phenotype is due to its inhibitory effect of Raf-MAPK signaling pathway (Fig. 4A and B). Regarding HGF-dependent PI3K-AKT signaling pathway, wortmannin weakly inhibited the wound closure in Huh7 cells and to the same extent by sorafenib in HepG2 cells (Supplementary Fig. 5). In contrast, wortmannin has no effect on Snail levels or on HCC morphology changes (Fig. 4A and B). Collectively, we speculate that activation of HGF-dependent PI3K-AKT pathway may not be involved in SNAI1 induction or morphologic change but at least partially involved in cell migration independent of Raf-MAPK-SNAI1 signaling.

Taken together, these results indicate that sorafenib inhibits the HGF-mediated EMT, which is characterized by cadherin switching, morphologic changes, and an increase in the cellular migrating phenotype, by inhibiting Raf-MAPK signaling, resulting in the downregulation of SNAI1 in HCC cells (Fig. 6).

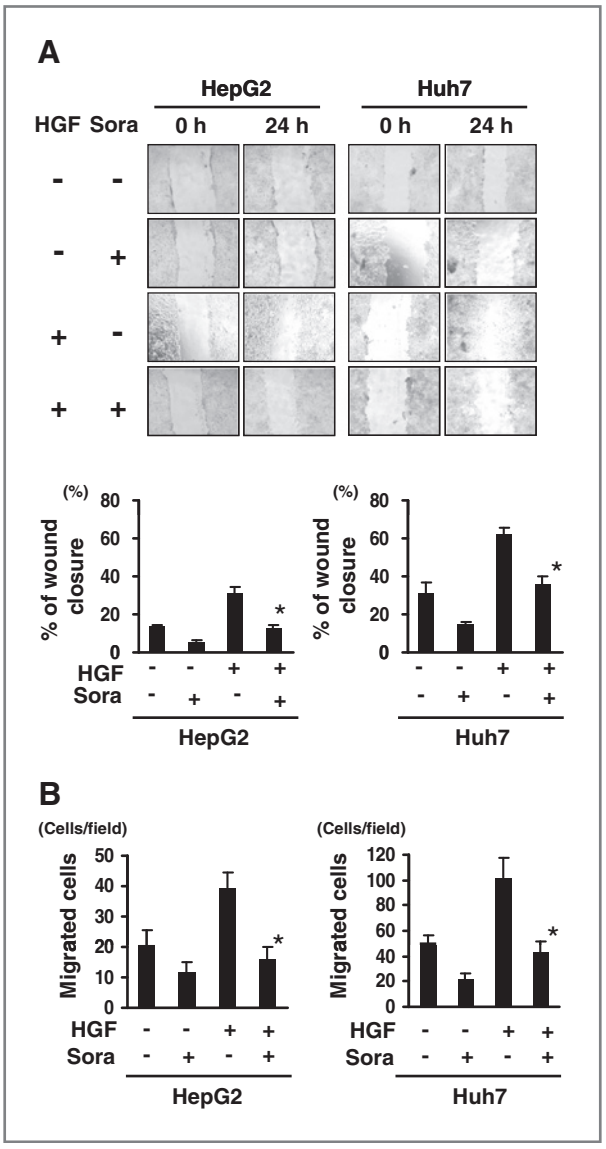

Figure 5. Sorafenib inhibits HGF-mediated cellular migration in HCC cells. A, a scratch assay revealed that HGF stimulation increased the cellular migration by about 2-fold, but sorafenib almost completely canceled the effect. The subconfluent HepG2 and Huh7 cells were scratched with a plastic pipette tip and incubated under the indicated conditions (control, 10 ng/mL of HGF; and HGF, 10 μmol/L of sorafenib). The scratch area was photographed and measured. The experiment was done in triplicate. *, sorafenib (–) versus (+), $P < 0.05$. B, migration assay using the Boyden chamber method revealed that sorafenib almost completely canceled the HGF-mediated cellular migration in both HCC cell lines. The cells were incubated under the indicated conditions: control, 10 ng/mL of HGF; and HGF, 10 μmol/L of sorafenib. *, sorafenib (–) versus (+), $P < 0.05$. Sora, sorafenib.

Discussion

Recent accumulating evidence has shown that the EMT is involved in drug sensitivity to several anticancer agents (25). Within this topic, the most intensively investigated drugs have been endothelial growth factor receptor (EGFR)–targeting drugs for the treatment of lung cancer. A clinical trial has revealed that lung cancer cells with strong E-cadherin expression exhibit a significantly longer time to progression after EGFR-TKI (tyrosine kinase inhibitor) treatment (26). Other studies on EGFR-targeting drugs have shown that mesenchymal type lung cancer cells exhibit an EMT-dependent acquisition of PDGFR, FGF receptor, and TGF-β receptor signaling pathways (27), and integrin-linked kinase is a novel target for overcoming HCC resistance to EGFR inhibition (28). Regarding sensitivity to gemcitabine, mesenchymal type cancer cells are reportedly associated with gemcitabine resistance in pancreatic cancer cells (29). The mechanism of resistance to gemcitabine has been shown to involve the activation of Notch signaling, which is mechanistically linked with the mesenchymal chemoresistance phenotype of pancreatic cancer cells (30). Thus, baseline cellular characteristics based on the EMT phenotype might be useful not only as prognostic biomarkers for a malignant phenotype but also as predictive markers

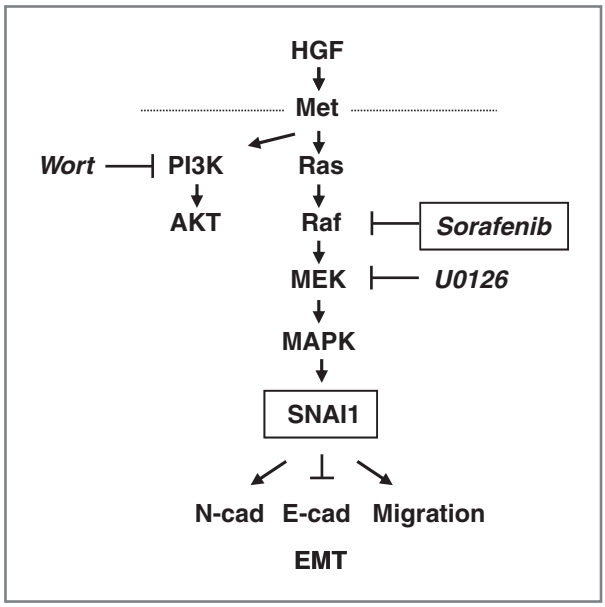

Figure 6. Diagram of the proposed mechanism by which sorafenib inhibits the EMT. Sorafenib inhibits the HGF-mediated EMT, which is characterized by morphologic changes, cadherin switching, and an increase in the cellular migrating phenotype. The anti-EMT effect of sorafenib occurs through the downregulation of SNAI1 by the inhibition of MAPK phosphorylation in HCC cells. Wort, wortmannin; N-cad, N-cadherin; E-cad, E-cadherin.

of sensitivity to anticancer agents. In this study, we focused on the signaling pathway responsible for inducing the EMT and showed that the multitarget TKI sorafenib downregulates SNAI1 by inhibiting Raf-MAPK signaling, thereby inhibiting the HGF-mediated EMT in HCC cells. Our findings may provide a novel insight into the actions of TKIs and their anti-EMT effects.

The mechanisms underlying the SNAI1-induced metastatic and aggressive phenotypes of cancer cells have recently been intensively investigated in both basic and clinical research studies. A novel aspect of the activity of SNAI1 is its involvement in immunosuppression. The SNAI1-induced EMT mediates regulatory T cells and impairs dendritic cells, accelerating cancer metastasis not only by enhancing invasion but also by inducing immunosuppression (31). A complex of histone deacetylase (HDAC) and SNAI1 plays an essential role in silencing E-cadherin (32), suggesting that the use of HDAC inhibitors to inhibit SNAI1 function might represent a promising therapeutic approach. On the other hand, large-scale clinical data on SNAI1 expression and the prognosis of patients with HCC were recently reported (33) and the overexpression of SNAI2 and/or TWIST was correlated with a worse prognosis. In contrast, no such significant differences were observed in samples that overexpressed SNAI2. The coexpression of Snail and TWIST was correlated with the worst prognosis for HCC (33). This evidence suggests that SNAI1 might be a useful therapeutic target for oncology. Our findings showed that sorafenib completely canceled the HGF-mediated SNAI1 induction in HepG2 and Huh7 cells. This activity of sorafenib, in addition to sorafenib's anti-angiogenic effects, might contribute to a clinical benefit against metastatic and aggressive phenotypes in patients with HCC.

Disclosure of Potential Conflicts of Interest

No potential conflicts of interest were disclosed.

Acknowledgments

We thank Tomoko Kitayama and the staff of the Life Science Research Institute for their technical assistance.

Grant Support

This work was supported in part by the Third-Term Comprehensive 10-Year Strategy for Cancer Control and a Grant-in-Aid for Cancer Research (H20-20-9) from the Ministry of Health and Labor Scientific Research Grants.

The costs of publication of this article were defrayed in part by the payment of page charges. This article must therefore be hereby marked *advertisement* in accordance with 18 U.S.C. Section 1734 solely to indicate this fact.

Received June 9, 2010; revised October 25, 2010; accepted October 25, 2010; published online January 10, 2011

References

1. Jemal A, Murray T, Ward E, et al. Cancer statistics, 2005. CA Cancer J Clin 2005;55:10–30.
2. Yamamoto J, Kosuge T, Takayama T, et al. Recurrence of hepatocellular carcinoma after surgery. Br J Surg 1996;83:1219–22.
3. Wilhelm SM, Carter C, Tang L, et al. BAY 43-9006 exhibits broad spectrum oral antitumor activity and targets the RAF/MEK/ERK pathway and receptor tyrosine kinases involved in tumor progression and angiogenesis. Cancer Res 2004;64:7099–109.
4. Llovet JM, Ricci S, Mazzaferro V, et al.; SHARP Investigators Study Group. Sorafenib in advanced hepatocellular carcinoma. N Engl J Med 2008;359:378–90.
5. Cheng AL, Kang YK, Chen Z,, et al. Efficacy and safety of sorafenib in patients in the Asia-Pacific region with advanced hepatocellular carcinoma: a phase III randomised, double-blind, placebo-controlled trial. Lancet Oncol 2009;10:25–34.
6. Peinado H, Olmeda D, Cano A. Snail, Zeb and bHLH factors in tumour progression: an alliance against the epithelial phenotype?Nat Rev Cancer 2007;7:415–28.
7. Hugo H, Ackland ML, Blick T, et al. Epithelial-mesenchymal and mesenchymal-epithelial transitions in carcinoma progression. J Cell Physiol 2007;213:374–83.
8. Tsuji T, Ibaragi S, Hu GF. Epithelial-mesenchymal transition and cell cooperativity in metastasis. Cancer Res 2009;69:7135–9.
9. Gentile A, Trusolino L, Comoglio PM. The Met tyrosine kinase receptor in development and cancer. Cancer Metastasis Rev 2008;27:85–94.
10. Eder JP, Vande Woude GF, Boerner SA, LoRusso PM. Novel therapeutic inhibitors of the c-Met signaling pathway in cancer. Clin Cancer Res 2009;15:2207–14.
11. Yang H, Magilnick N, Noureddin M, Mato JM, Lu SC. Effect of hepatocyte growth factor on methionine adenosyltransferase genes

and growth is cell density-dependent in HepG2 cells. J Cell Physiol 2007;210:766–73.
12. Mizuguchi T, Nagayama M, Meguro M, et al. Prognostic impact of surgical complications and preoperative serum hepatocyte growth factor in hepatocellular carcinoma patients after initial hepatectomy. J Gastrointest Surg 2009;13:325–33.
13. Chau GY, Lui WY, Chi CW, et al. Significance of serum hepatocyte growth factor levels in patients with hepatocellular carcinoma undergoing hepatic resection. Eur J Surg Oncol 2008;34:333–8.
14. Yamagamim H, Moriyama M, Matsumura H, et al. Serum concentrations of human hepatocyte growth factor is a useful indicator for predicting the occurrence of hepatocellular carcinomas in C-viral chronic liver diseases. Cancer 2002;95:824–34.
15. Tanaka K, Arao T, Maegawa M, et al. SRPX2 is overexpressed in gastric cancer and promotes cellular migration and adhesion. Int J Cancer 2009;124:1072–80.
16. Matsumoto K, Arao T, Tanaka K, et al. mTOR signal and hypoxia-inducible factor-1 alpha regulate CD133 expression in cancer cells. Cancer Res 2009;69:7160–4.
17. Kaneda H, Arao T, Tanaka K, et al. FOXQ1 is overexpressed in colorectal cancer and enhances tumorigenicity and tumor growth. Cancer Res 2010;70:2053–63.
18. Lee JM, Dedhar S, Kalluri R, Thompson EW: The epithelial-mesenchymal transition: new insights in signaling, development, and disease. J Cell Biol 2006;172:973–81.
19. Wheelock MJ, Shintani Y, Maeda M, Fukumoto Y, Johnson KR. Cadherin switching. J Cell Sci 2008;121:727–35.
20. Lo HW, Hsu SC, Xia W, et al. Epidermal growth factor receptor cooperates with signal transducer and activator of transcription 3 to induce epithelial-mesenchymal transition in cancer cells via up-regulation of TWIST gene expression. Cancer Res 2007;67:9066–76.
21. Vincent T, Neve EP, Johnson JR, et al. A SNAIL1-SMAD3/4 transcriptional repressor complex promotes TGF-beta mediated epithelial-mesenchymal transition. Nat Cell Biol 2009;11:943–50.
22. Larue L, Bellacosa A. Epithelial-mesenchymal transition in development and cancer: role of phosphatidylinositol 3' kinase/AKT pathways. Oncogene 2005;24:7443–54.
23. Zavadil J, Böttinger EP. TGF-beta and epithelial-to-mesenchymal transitions. Oncogene 2005;24:5764–74.
24. Liu L, Cao Y, Chen C, et al. Sorafenib blocks the RAF/MEK/ERK pathway, inhibits tumor angiogenesis, and induces tumor cell apoptosis in hepatocellular carcinoma model PLC/PRF/5. Cancer Res 2006;66:11851–8.
25. Voulgari A, Pintzas A. Epithelial-mesenchymal transition in cancer metastasis: mechanisms, markers and strategies to overcome drug resistance in the clinic. Biochim Biophys Acta 2009;1796:75–90.
26. Yauch RL, Januario T, Eberhard DA, et al. Epithelial versus mesenchymal phenotype determines *in vitro* sensitivity and predicts clinical activity of erlotinib in lung cancer patients. Clin Cancer Res 2005; 11:8686–98.
27. Thomson S, Petti F, Sujka-Kwok I, Epstein D, Haley JD. Kinase switching in mesenchymal-like non-small cell lung cancer lines contributes to EGFR inhibitor resistance through pathway redundancy. Clin Exp Metastasis 2008;25:843–54.
28. Fuchs BC, Fujii T, Dorfman JD, et al. Epithelial-to-mesenchymal transition and integrin-linked kinase mediate sensitivity to epidermal growth factor receptor inhibition in human hepatoma cells. Cancer Res 2008;68:2391–9.
29. Arumugam T, Ramachandran V, Fournier KF, et al. Epithelial to mesenchymal transition contributes to drug resistance in pancreatic cancer. Cancer Res 2009;69:5820–8.
30. Wang Z, Li Y, Kong D, et al. Acquisition of epithelial-mesenchymal transition phenotype of gemcitabine-resistant pancreatic cancer cells is linked with activation of the notch signaling pathway. Cancer Res 2009;69:2400–7.
31. Kudo-Saito C, Shirako H, Takeuchi T, Kawakami Y. Cancer metastasis is accelerated through immunosuppression during Snail-induced EMT of cancer cells. Cancer Cell 2009;15:195–206.
32. von Burstin J, Eser S, Paul MC, et al. E-cadherin regulates metastasis of pancreatic cancer *in vivo* and is suppressed by a SNAIL/HDAC1/HDAC2 repressor complex. Gastroenterology 2009;137:361–71.
33. Yang MH, Chen CL, Chau GY, et al. Comprehensive analysis of the independent effect of Twist and Snail in promoting metastasis of hepatocellular carcinoma. Hepatology 2009;50:1464–74.